Investigation on Wearable Airbags for Motorcyclists through Simulations and Experimental Tests

Edoardo Marconi, Franco Gatto and Matteo Massaro

Abstract Software for the simulation of airbags has been available for more than three decades and today is widely used in the automotive industry. Nonetheless, since the introduction of the first wearable airbags for motorcycle riders in the late 1990s, these numerical tools have seen only little application in this fairly new field. The objective of this research is to assess the performance of wearable airbag systems for motorcyclists through experimental tests and numerical simulation. Virtual models are created for two typical test set-ups and numerical results are compared against the corresponding experimental findings. The first test considered is the drop test, derived from the set-up used in EN 1621 for the certification of protectors and employed here to calibrate the finite element airbag model. The second test scenario is the thorax impact test, described in 49 CFR 572 (high-speed test) and SAE J2779 (low-speed test). This set-up, in which the airbag is fitted to a Hybrid III 50th dummy, is used to assess the airbag's performance in terms of reduction of peak chest deflection and to carry out a parametric analysis on the main airbag parameters: inflation pressure and inflated thickness.

Key words: 49 CFR 572, drop test, EN 1621, Hybrid III 50th, motorcycle safety, simulation, thorax impact test, wearable airbag

Edoardo Marconi
Dept. of Industrial Engineering, University of Padova, Via Venezia 1, 35131 Padova, Italy. e-mail: edoardo.marconi@phd.unipd.it

Franco Gatto
Dainese SpA, Via dell'Artigianato 35, 36060 Molvena, Italy. e-mail: franco.gatto@dainese.it

Matteo Massaro
Dept. of Industrial Engineering, University of Padova, Via Venezia 1, 35131 Padova, Italy. e-mail: matteo.massaro@unipd.it

1 Introduction

Airbag systems first appeared in production cars in the US in the 1970s and are now a standard equipment in most cars [11, 17, 19]. Numerical simulation is a customary tool when it comes to the development of airbags for the car industry, see e.g. [13, 21].

Airbag systems have appeared only very recently on production motorcycles. The first one appeared in 2006 on the Honda Gold Wing, with the aim of mitigating the consequences of frontal collisions. Some of the experimental investigations related to such airbag were published in the late 1990s [12, 20], while numerical simulations were later reported [15]. More recently a new concept of airbag mounted on a motorcycle has been presented [1, 2]. This system differs from the former because the airbag does not need a support system or reaction structure in place during deployment. The possible application of frontal airbag to smaller motorcycles has been discussed in [4, 14]. Research on airbags mounted on motorcycles were also reported by Yamaha [9]: both sled and full scale tests with related simulation were reported - in this case the airbag was installed on the front-end of the rider's seat and supported by a back-plate. Finally in [5], a frontal airbag system is tested and simulated on a three-wheeled vehicle, again the focus is on frontal collision.

Wearable airbags are another option when it comes to the protection of motorcycle riders. One of the advantages is the possibility of protecting riders in low-side and high-side crashes [6, 7] and oblique collision, where frontal airbags mounted on the motorcycle would clearly be not effective. There are two main activation systems in the case of wearable airbags: mechanical (a wire connecting the bike and the rider is pulled when the rider falls) and electronic (accelerometers and/or gyrometers on the bike and/or on the rider detect the fall and trigger the airbag activation). Among the advantages of mechanical activation are simplicity and robustness when it comes to activation (when the wire is pulled the system triggers the airbag, while an electronic system relies on a fall detection algorithm that could fail the detection of some falls). Among the disadvantages are the possible interference between the rider and the activation wire and the need for the rider to fall 'enough' to pull the wire and trigger the activation. A number of systems of this kind have been available on the market since the late 1990s, e.g. [25, 29, 31, 32, 33]. On the other side there are systems based on electronic activation, i.e. on algorithms that detect the fall using some 'function' computed from the sensors output, see e.g. [3, 8]. The first airbag of this kind was made available by Dainese in 2007 for race riders [27] and in 2011 as a commercial product [28]. As of today, there are only few other race [22, 30] and road [23, 26] products of this type. From 2018 airbags fitted on race rider's suits are compulsory within the FIM MotoGP World Championship.

Most of the development of wearable airbags for motorcycle rider suits has been experimental [16]. The present work aims at simulating the performance of a wearable airbag system for motorcycle riders using numerical simulation through the code Madymo. Two scenarios are considered: the drop test and the thorax impact test. The former is used to estimate bag material properties, while the second is used to assess the performance of the airbag system. Finally, a parametric investigation on the main airbag characteristics is carried out. The simulations and tests have been performed using the Hybrid III 50th dummy model. In this study the pressure within the airbag volume is assumed constant (although time-varying) – this is a good assumption in the case the inflation process is not the main focus of the analysis – and the airbag is assumed perfectly inflated at the instant of impact.

The work is organized as follows. In Sect. 2 the drop test for the identification of the main airbag parameters is described. In Sect. 3 the thorax tests, with and without airbag, are presented and compared against experimental findings for the validation of the numerical model. Finally, in Sect. 4 a parametric analysis on the main airbag parameters is carried out using both low-speed and high-speed thorax tests. Some of the results presented are normalized for confidentiality reasons.

2 Drop test

The drop test is considered in EN 1621, namely Part 4 (*Motorcyclists' inflatable protectors – Requirements and test methods*), for the certification of mechanically activated airbag systems. However, certification bodies often make use of the same requirements also for electronically activated systems [10]. In the test, a striker falls on the protector, which is on top of an anvil attached to a force transducer. The main outcome of the test is the peak force transmitted to the anvil, which determines the certified level of protection.

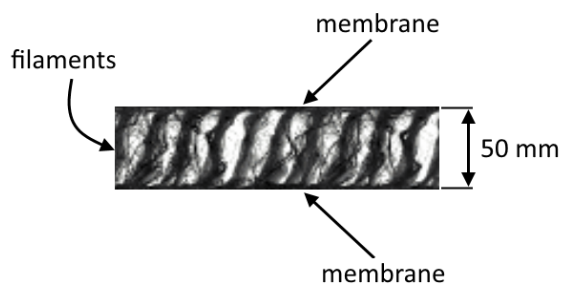

Fig. 1: Airbag section view: the inner filaments connect the two membranes in order to obtain a flat shape of the airbag once it is inflated.

The airbag considered in this research is made up of two membranes stitched on the edges. Each membrane consists of a thermoplastic material and a fabric material, plus internal filaments of the fabric material, see Fig. 1, that are in tension when the airbag is inflated. When the airbag is inflated, some of these inner filaments are slightly inclined and thus contribute to the planar stiffness of the membrane. Because of the complexity of the material employed, simple tests on the sole membrane element proved not suitable to obtain the mechanical characteristics of the airbag (e.g. missed stiffening effect). It was then decided to perform a number of drop tests on the airbag at the nominal inflation pressure, both numerically and experimentally, in order to identify the main material properties. The virtual model of the experimental set-up is shown in Fig. 2. A square 0.6×0.6 m bag was used. Both impactor and anvil were hemispherical, 0.1 m in diameter: this geometry, without sharp edges, does not damage the bag material, thus allowing multiple tests. Due to the geometry of the bag, reduced impact energy values have been chosen, in order to avoid direct impact between impactor and anvil.

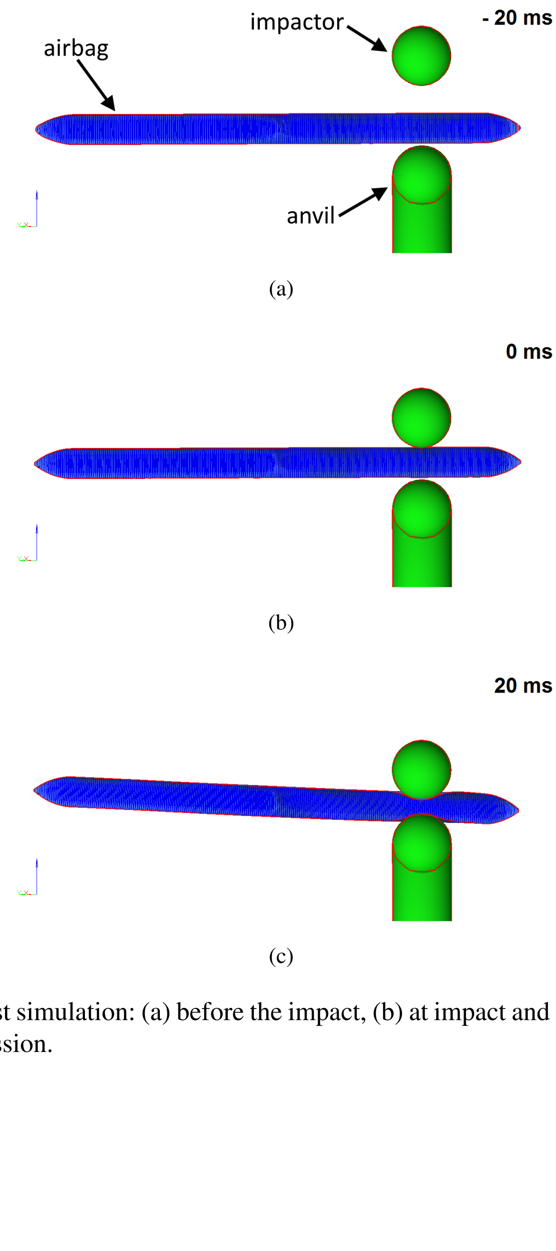

Fig. 2: Drop test simulation: (a) before the impact, (b) at impact and (c) at maximum airbag compression.

The bag is discretized using membrane elements, whose maximum size is 20 mm (reduction of the size down to 5 mm did not show significant variations in the results), while the filaments are modelled through spring-damper elements. For simplicity, the material model selected for this study is linear-isotropic, i.e.

$$\sigma = S\varepsilon + \gamma\dot{\varepsilon}, \tag{1}$$

where σ is the stress vector, ε the strain vector, $\dot{\varepsilon}$ the strain rate vector, S is the well known stiffness matrix for linear-isotropic materials (which depends on the Young modulus and Poisson ratio only), and γ is a rate sensitivity parameter. The latter is defined as

$$\gamma = Ed\Delta t_e, \tag{2}$$

where E is the Young modulus, d is a damping factor and Δt_e is the element time step, i.e. the time required for a sound wave to cross the element – undamped Courant time step. The integration time step Δt employed is the minimum of all Δt_e, scaled down by the factor $(\sqrt{d^2+1} - d)$ to account for the effect of damping that reduces the maximum step size allowed for stability [18]. In this study the damping factor is $d = 0.2$ (after simulation over a wide range of values showed negligible effects) and the Poisson ratio is zero (again after simulations over a wide range of values). The parameters for the filaments are their stiffness k and damping coefficient c – both assumed constant

$$F = k\Delta l + c\dot{\Delta l}, \tag{3}$$

where F is the force resulting from deflection Δl and deflection rate $\dot{\Delta l}$. Actually, the meaningful parameter for the filaments is the stiffness per unit area: from this value, the stiffness of the single filament is obtained.

Different drop tests have been simulated and compared to the experimental findings in order to obtain such parameters. The values of the damping coefficients, for both the membrane elements and the inner filaments, proved not significant: the peak and shape of the anvil force is minimally affected by the damping. The stiffness of the inner filaments affects the transmitted force only at very low values and then quickly saturates over a certain threshold, see Fig. 3. This is because, for a given inflation pressure, low stiffness filaments deform significantly, allowing a higher distance between the two membranes and thus changing the reference geometry of the airbag; see Fig. 4. This behaviour was not observed on the real airbag, which maintains a constant thickness in a wide range of inflation pressure. For this reason, the filaments' linear stiffness was chosen in the saturation range, in which the height of the airbag and the transmitted force remains constant.

The last parameter that needs to be determined is the Young modulus of the membrane elements. The results of the analysis are reported in Fig. 5. This was found to be the parameter with the largest influence on the force transmitted to the anvil in the drop test. In order to find a suitable value for modelling the behaviour of the real airbag in an impact, the Young modulus was determined by matching the

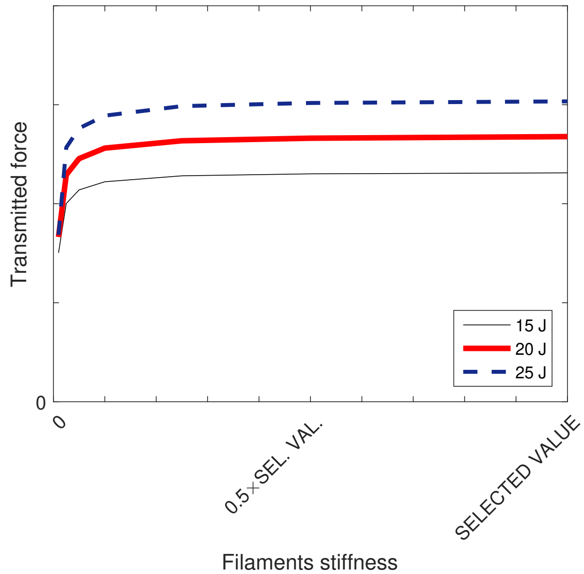

Fig. 3: Effect of filament stiffness on the peak of the transmitted force. The softer the filaments, the lower the transmitted force (until saturation). The selected value is inside the saturation range, in which increasing filament stiffness no longer affects the transmitted force and the inflated airbag thickness.

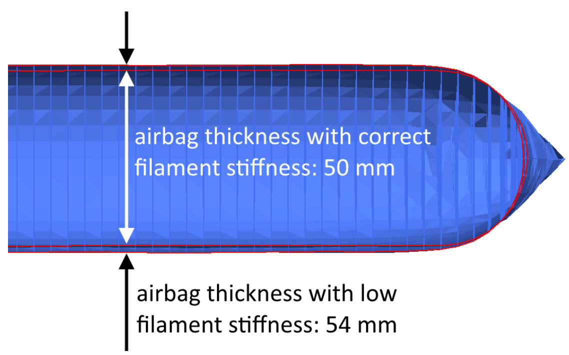

Fig. 4: Difference in inflated airbag geometry caused by different filament stiffness. Softer filaments result in a thicker inflated airbag shape, also affecting force transmission (Fig. 3).

peak of the transmitted force calculated in the simulations with that obtained in the experimental test.

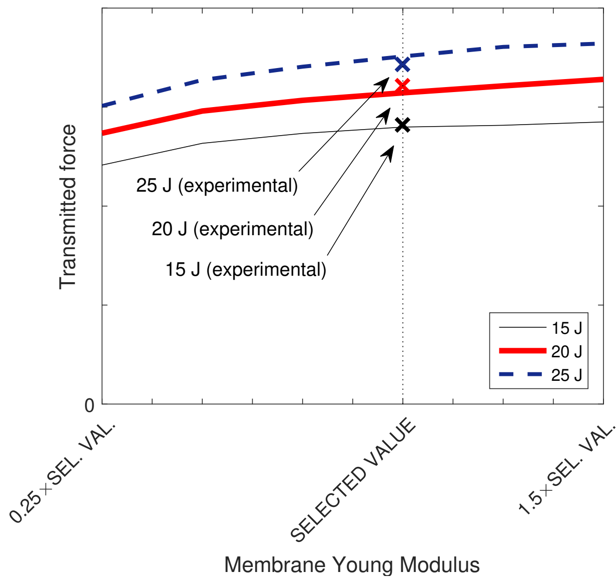

Fig. 5: Effect of membrane Young modulus on the peak of the transmitted force. The stiffer the membrane, the higher the transmitted force. Cross markers represent the experimental values for each energy level.

Summarizing, at the end of the drop test campaign the elastic modulus of the membrane, the stiffness of the filaments and the damping coefficients of the airbag are available.

3 Thorax impact test

The thorax impact test is considered in 49 CFR 572, for the certification and calibration of dummies. This test is considered especially relevant for the assessment of the performance of thorax protectors such as wearable airbags. The simulated test reproduced the corresponding experimental test previously carried out. A 0.1524 m diameter cylindrical pendulum of mass 23.36 kg hits the chest of an instrumented dummy at a velocity of 6.7 m/s. The dummy is placed on a flat, smooth, horizontal steel surface and can thus slide during the impact. In order to pass the test, the measured chest deflection has to lay in the interval 0.0635-0.0726 m. This test configuration (see Fig. 6) was chosen as the most meaningful and reproducible to verify the performance of a new chest protector during the APROSYS project [24]. As the chest is one of the areas covered by most wearable airbags intended for road use, this test method was also identified as one of the tools to assess the performance of inflatable protectors on this part of the body.

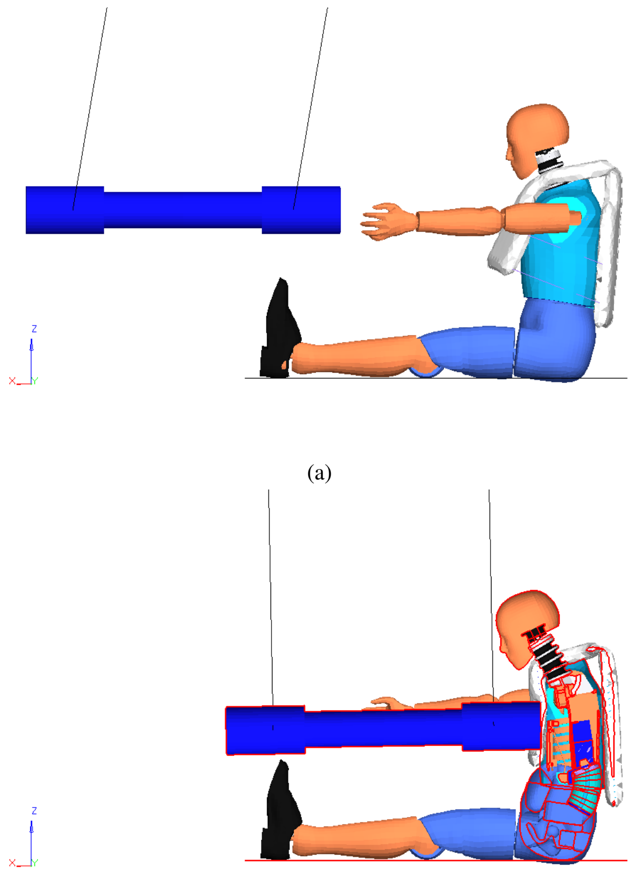

(a)

(b)

Fig. 6: Thorax impact test virtual model: (a) after airbag inflation and before impactor release, (b) section view at maximum chest deflection.

Preliminary steps for the simulation of the thorax impact test involve the modelling, meshing and fitting of the virtual airbag to the dummy model. The selected dummy is a Hybrid III 50th Percentile, which is the same used in the full scale experimental test. The airbag was first modelled as a flat 'shell' element. Then its shape was adapted to the body of the dummy through the application of acceleration fields to the finite elements that make up the airbag numerical model. This process is repeated in multiple steps, as depicted in Fig. 7, each time adapting direction, intensity and region of application of the acceleration fields, until a satisfactory shape of the airbag is obtained. Alternative techniques can also be adopted, depending on the shape of the airbag and the body areas it has to cover.

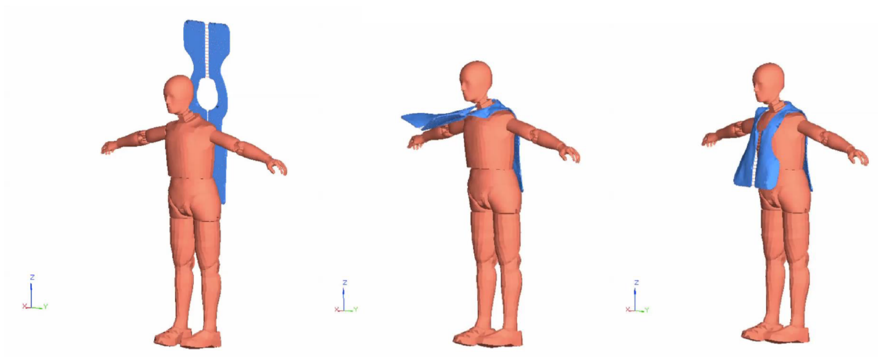

Fig. 7: Fitting process based on accelerations fields to obtain the initial shape of the airbag finite element model – the final step before simulation will involve the addition of the side straps and back connections shown in Fig. 8.

In the next step, the airbag needs to be linked to the dummy in order to prevent its motion when inflated and ensure it is hit by the impactor during the test. In the real system this is achieved accommodating the bag inside a technical jacket or integrating the bag in a vest worn over the jacket. In the virtual model, it is important that the connection fulfils its function of keeping the airbag in the right position, but at the same time it should not alter the interaction between dummy and airbag. To attain such result, two couples of symmetrical nodes (one on each of the two chambers) on the rear part of the airbag were connected to two point on the back of the dummy through visco-elastic constraints. Furthermore, four additional one-dimensional elements ('side straps') were added to the finite element model to link the front and rear parts of the airbag. This is necessary because, as the internal pressure increases during the inflation process, the airbag tends to straighten up, losing its correct shape. The resulting shape of the inflated airbag model in shown in Fig. 8, where the side straps are clearly visible.

At this point, the model can be simulated. Among the many outputs that can be monitored, the focus is on the chest deflection, which is also used for the certification of dummies. The standard test, which does not include the airbag, gives a chest deflection signal very close to that obtained in the experimental test, with a slightly lower peak value (-3%) in the simulation, see Fig. 9a. This result confirms that the numerical model of the dummy and the experimental set-up have been built correctly. The simulation with the airbag fitted to the dummy shows again a chest deflection signal qualitatively similar to the experimental one, this time with a larger

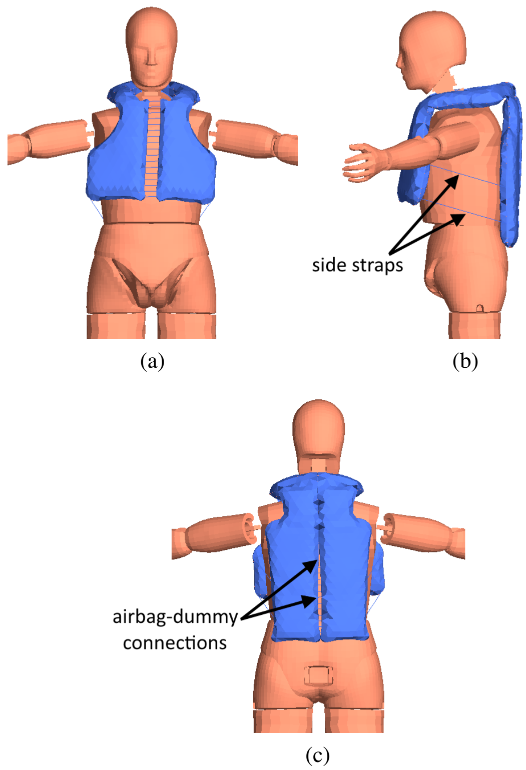

Fig. 8: Airbag finite element model fitted to the Hybrid III 50th dummy: (a) front view; (b) side view (the side straps are highlighted); (c) rear view (the connections between airbag and dummy are highlighted).

peak value (+7%) in the simulation when compared to the actual test, see Fig. 9b. In other words, the virtual airbag proves a little less protective than the real device, reducing the peak chest deflection by 18% instead of 26%. The differences found between simulation and real tests are reasonably small and can be considered satisfactory – in addition the simulation results are conservative. At this stage, the virtual airbag model is considered validated.

4 Parametric analysis

The effect of the main parameters on the airbag response has been investigated using the virtual model validated in the previous section. Two characteristics, potentially alterable also in the real product, have been considered: the inflation pressure, which is varied by changing the total mass of gas used to inflate the bag, and the thickness

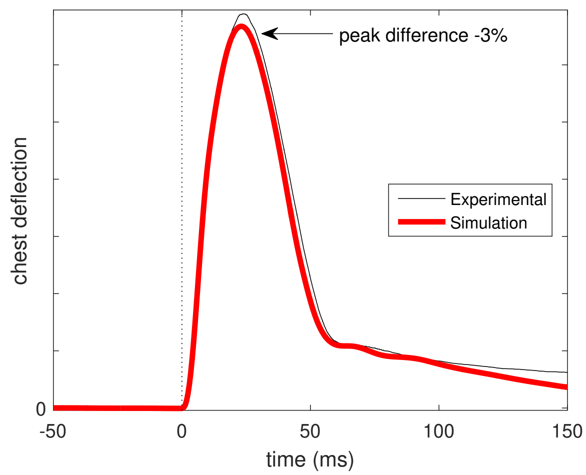

(a)

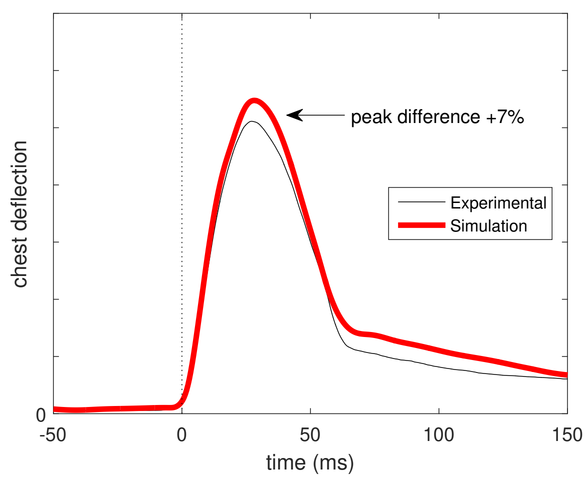

(b)

Fig. 9: Chest deflection as a function of time: a) without airbag; b) with airbag. The dotted line highlights the beginning of the impact (time zero).

of the inflated bag, that can be adjusted by changing the length of the inner filaments. Moreover, in addition to the standard thorax impact test, its low-speed variant SAE J2779 (*Low Speed Thorax Impact Test Procedure for the HIII 50th Male Dummy*) was simulated. The same set-up used in 49 CFR 572 is employed, but the impactor speed is reduced to 3 m/s. This low-speed test was created to satisfy the demand for a calibration test where the energy involved is comparable to an actual low energy automotive impact test.

Fig. 10a and Fig. 10b report the effect of the inflation pressure and airbag thickness on the peak chest deflection, for the low-speed and the high-speed tests respectively. With the aim of minimizing the peak chest deflection, an optimal value of inflation pressure can be found for given impactor speed and airbag inflated thickness. The following physical interpretation can explain the existence of such optimal value. For pressures below the optimal one, the impactor fully compresses the airbag and hits the dummy's chest. In this range, an increase in the airbag pressure reduces the impactor deceleration and its relative velocity when it impacts the chest. On the other hand, above the optimal value, an increase in the airbag pressure reduces the airbag compression when it is hit by the impactor, and thus the impactor deceleration is more rapid, resulting in a higher peak chest deflection. At high pressures the response becomes almost constant, with a chest deflection lower than that obtained without airbag, since the load is distributed over a larger area. Ultimately, the optimal pressure that minimizes the peak chest deflection is the lowest value sufficient to prevent the impactor from hitting the chest, after full compression of the airbag. In the low-speed scenario, the variation in the peak chest deflection between the optimal pressure and the high pressure (when saturation occurs) is around 17% in the case of 65 mm thickness and 26% in the case of 35 mm thickness. In the high-speed scenario, the difference is 12% and 6% for 65 mm and 35 mm respectively. Therefore the low speed condition with the low thickness airbag is the scenario most sensitive to pressure optimisation.

Analysing the effect of the other parameters, it can be observed that the higher the airbag inflated thickness, the lower the optimal pressure for a given impactor velocity. In addition, lower peak chest deflection values correspond to higher inflated thickness values at each pressure: this means that, regardless the pressure, choosing the highest thickness allowed by the ergonomic constraints is always advantageous.

It can also be noticed that, as intuition would suggest, higher impact energies (i.e. higher impactor velocities) require a higher inflation pressure to minimize the peak chest deflection, given the inflated thickness of the airbag.

5 Conclusions

The performance of a wearable airbag system intended for the protection of motorcycle riders has been studied through modelling and simulation of two test set-ups. The drop test has allowed the calibration of the airbag finite element model, determining the mechanical properties of the airbag material that most closely fit the ex-

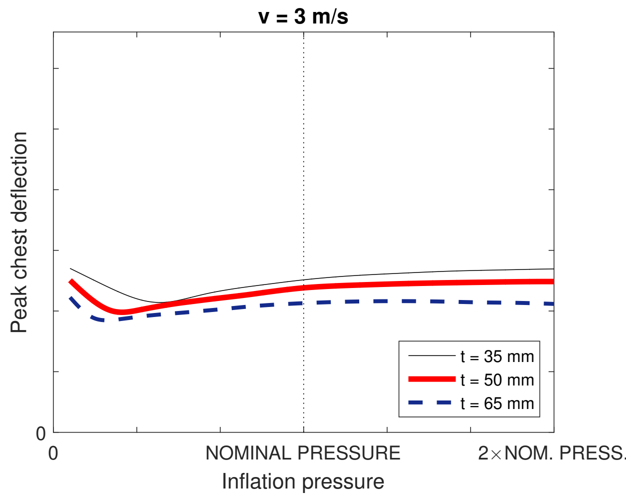

(a)

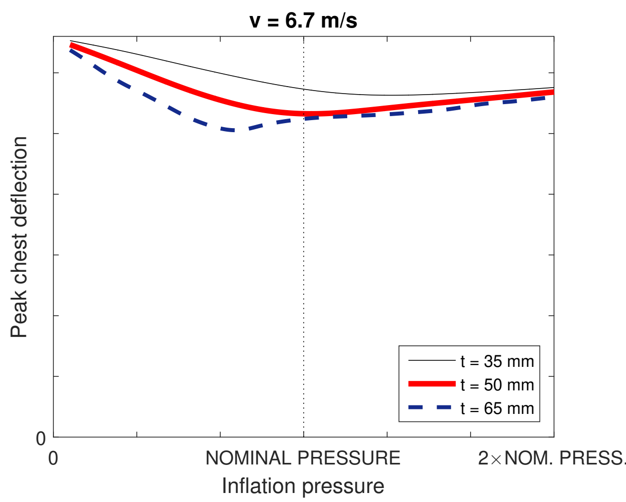

(b)

Fig. 10: Effect of airbag inflated thickness and inflation pressure on peak chest deflection: a) low-speed thorax impact test; b) high-speed thorax impact test. Each curve shows a minimum, corresponding to the optimal inflation pressure for the given condition (impact speed and airbag thickness).

perimental outcomes. A linear-isotropic material model has been employed. Then, the airbag model has been validated using the thorax impact test. The simulation proved reasonably close to the experimentation, with 7% maximum difference in the chest deflection signal. The same setup has been used to perform a parametric analysis in order to investigate the effect of inflation pressure and airbag thickness on the performance of the airbag. With the aim of minimizing the peak chest deflection, an optimal inflation pressure exists, which is higher for higher impact energy and for lower airbag thickness; moreover, high airbag thickness is always advantageous.

References

1. Aikyo Y, Kobayashi Y, Akashi T, Ishiwatari M (2015) Feasibility study of airbag concept applicable to motorcycles without sufficient reaction structure. Traffic Inj Prev 16.sup1:S148–S152.
2. Aikyo Y, Kobayashi Y, Sato T, Akashi T, Ishiwatari M (2016) Study on airbag concept for motorcycles using opposing vehicle as reaction structure. SAE Technical Paper no. 2015-32-0813.
3. Ambrogi A, Bellati A, Cossalter V, Lot R (2008) Method and device for the prediction of a fall of a person from a vehicle or the like. Pat. EP, 2079613:B1, .
4. Ariffin AH, Rahman MK, Hamzah A, Paiman NF, Isa MHM, Solah MS, Jawi ZM, Kassim KAA (2013) Exploratory study on airbag suitability for small engine capacity motorcycle in Malaysia. In: Malaysian Universities Transport Research Forum Conference.
5. Barbania D, Baldanzini N, Pierini M, Santucci M (2012) Analisi e sviluppo di un modello FEM di airbag integrato su motoveicolo (Analysis and development of a FEM model of an airbag integrated on a motorcycle). In: AIAS – Associazione Italiana per l'Analisi delle Sollecitazioni 41 Convegno nazionale, 5-8 Settembre 2012, Universit degli Studi di Padova.
6. Cossalter V (2006) Motorcycle dynamics. Lulu.com.
7. Cossalter V, Bellati A, Cafaggi V (2005) Exploratory study of the dynamic behaviour of motorcycle-rider during incipient fall events. In: In the 19th International Technical Conference on the Enhanced Safety of Vehicles Conference (ESV) in Washington, DC. pp.6–9.
8. Cossalter V, Aguggiaro A, Debus D, Bellati A, Ambrogi A (2007) Real cases motorcycle and rider race data investigation: fall behavior analysis. In: Proceedings of the 20th International Technical Conference on Enhanced Safety of Vehicles: Innovations for Safety Opportunities and Challenges, Lyon, France. pp.18–21.
9. Deguchi M, Kanbe S, Hannya Y (2007) Basic research for motorcycle crashworthiness and a new airbag system. SAE Technical Paper no. 2007-32-0106.
10. European Commission (1989) Personal protective equipment (PPE). 89/686/EEC.
11. Hoye A (2010) Are airbags a dangerous safety measure? A meta-analysis of the effects of frontal airbags on driver fatalities. Accid Anal Prev 2030–2040.
12. Iijima S, Hosono S, Ota A, Yamamoto T (1998) Exploratory study of an airbag concept for a large touring motorcycle. In: 16th International Technical Conference on the Enhanced Safety of Vehicles.
13. Khan MU, Moatamedi M (2008) A review of airbag test and analysis. Int J Crashworthiness 13.1:67–76.
14. Kobayashi Y, Makabe T (2013) Crash detection method for motorcycle airbag system with sensors on the front fork. In: 23rd International Technical Conference on the Enhanced Safety of Vehicles.
15. Kuroe T, Namiki H, Iijima S (2005) Exploratory study of an airbag concept for a large touring motorcycle: further research second report. In: 19th International Technical Conference on the Enhanced Safety Vehicles.

16. Marconi E, Gatto F, Massaro M (2018) Numerical and Experimental Assessment of the Performance of Wearable Airbags for Motorcycle Riders. In: Lecture Notes in Engineering and Computer Science: Proceedings of The World Congress on Engineering 2018, 4-6 July, 2018, London, U.K., pp805-810
17. Runge JW (2010) Special crash investigations: a model for future corrective action. Ann Emerg Med.
18. TASS International (2015) Madymo Theory Manual. Version 7.6.
19. Thompson K, Segui-Gomez M, Graham J (1999) Validating analytical judgments: the case of the airbag's lifesaving effectiveness. Reliab Eng Syst Safe 66:57–68.
20. Yamazaki T, Iijima S, Yamamoto T (2001) Exploratory study of an airbag concept for a large touring motorcycle: further research. In: 17th International Technical Conference on the Enhanced Safety of Vehicles.
21. Zhang H, Raman S, Gopal M, Han T (2004) Evaluation and comparison of CFD integrated airbag models in LS-DYNA, MADYMO and PAM-CRASH. SAE Technical Paper no. 2004-01-1627.
22. Alpinestars - Tech-Air Race Airbag System. `https://www.alpinestars.com/tech-air-race-airbag-system`. Accessed: 2018-03-26.
23. Alpinestars - Tech-Air Street Airbag System. `https://www.alpinestars.com/tech-air-street-airbag-system`. Accessed: 2018-03-26.
24. APROSYS - Advanced Protection Systems (6th RTD EU Frame Programme). `https://trimis.ec.europa.eu/project/advanced-protection-systems`. Accessed: 2018-03-26.
25. Bering - C-Protect Air. `http://www.bering.fr/airbag/cpa.html?___store=english&___from_store=english`. Accessed: 2018-03-26.
26. Bering - Protect Air. `http://www.bering.fr/airbag/protect-air.html?___store=english&___from_store=english`. Accessed: 2018-03-26.
27. Dainese D-Air - Airbag System for Racers. `https://www.dainese.com/d-air/racers/`. Accessed: 2018-03-26.
28. Dainese D-Air - Airbag System for Riders. `https://www.dainese.com/d-air/riders/`. Accessed: 2018-03-26.
29. Helite motorcycle airbags - from MotoGP vests to road jackets. `https://www.helite.com/airbag-motorcycle`. Accessed: 2018-03-26.
30. In&motion - MotoGP. `https://www.inemotion.com/moto/`. Accessed: 2018-03-26.
31. Motoairbag - Airbags for motorcyclists. `http://www.motoairbag.com/welcome`. Accessed: 2018-03-26.
32. Rewin Air Impact. `http://www.rewin.it/main.php?pagina=cataindx&radice=AIRIMPACT&lingua=eng`. Accessed: 2018-03-26.
33. Spidi - Motorcycle Airbag Neck Protector. `https://www.spidi.com/eu_en/products/safety/airbag.html?&genere[]=2741&genere[]=2739`. Accessed: 2018-03-26.